THE JOURNAL OF BIOLOGICAL CHEMISTRY VOL. 284, NO. 15, pp. 10160–10173, April 10, 2009

ERp57 Does Not Require Interactions with Calnexin and Calreticulin to Promote Assembly of Class I Histocompatibility Molecules, and It Enhances Peptide Loading Independently of Its Redox Activity*

Received for publication, November 3, 2008, and in revised form, January 26, 2009 Published, JBC Papers in Press, February 5, 2009, DOI 10.1074/jbc.M808356200

Yinan Zhang[‡], Guennadi Kozlov[§], Cosmin L. Pocanschi[‡], Ulf Brockmeier[‡], Breanna S. Ireland[‡], Pekka Maattanen[§], Chris Howe[¶], Tim Elliott[¶], Kalle Gehring[§], and David B. Williams[‡1]

From the [‡]Departments of Biochemistry and Immunology, University of Toronto, Toronto M5S 1A8, Canada, the [§]Department of Biochemistry, McGill University, Montréal H3G 1Y6, Canada, and the [¶]Cancer Sciences Division, University of Southampton School of Medicine, Southampton SO16 6YD, United Kingdom

ERp57 is a thiol oxidoreductase that catalyzes disulfide formation in heavy chains of class I histocompatibility molecules. It also forms a mixed disulfide with tapasin within the class I peptide loading complex, stabilizing the complex and promoting efficient binding of peptides to class I molecules. Since ERp57 associates with the lectin chaperones calnexin and calreticulin, it is thought that ERp57 requires these chaperones to gain access to its substrates. To test this idea, we examined class I biogenesis in cells lacking calnexin or calreticulin or that express an ERp57 mutant that fails to bind to these chaperones. Remarkably, heavy chain disulfides formed at the same rate in these cells as in wild type cells. Moreover, ERp57 formed a mixed disulfide with tapasin and promoted efficient peptide loading in the absence of interactions with calnexin and calreticulin. These findings suggest that ERp57 has the capacity to recognize its substrates directly in addition to being recruited through lectin chaperones. We also found that calreticulin could be recruited into the peptide loading complex in the absence of interactions with both ERp57 and substrate oligosaccharides, demonstrating the importance of its polypeptide binding site in substrate recognition. Finally, by inactivating the redox-active sites of ERp57, we demonstrate that its enzymatic activity is dispensable in stabilizing the peptide loading complex and in supporting efficient peptide loading. Thus, ERp57 appears to play a structural rather than catalytic role within the peptide loading complex.

Major histocompatibility complex (MHC)[2] class I molecules present antigenic peptides to cytotoxic T lymphocytes (CTL), which leads to the elimination of virus-infected cells. MHC class I molecules are heterotrimers consisting of a transmembrane heavy chain (H chain), a soluble subunit termed β_2-microglobulin (β_2m), and a peptide ligand of 8–10 residues. Assembly of class I molecules begins in the endoplasmic reticulum (ER), where the glycosylated H chain binds to the membrane-bound lectin chaperone calnexin (Cnx) and its associated thiol oxidoreductase, ERp57. At this early stage, the two highly conserved disulfide bonds within the H chain are formed, and the H chain assembles with β_2m. H chain-β_2m heterodimers then enter a peptide loading complex (PLC), where class I molecules acquire peptides for display to CTL. The PLC consists of calreticulin (Crt), the soluble paralog of Cnx, an associated ERp57 molecule, a peptide transporter termed TAP, and tapasin, which is the nucleus of the PLC, bridging the interaction between class I heterodimers and the TAP peptide transporter. Once peptides are translocated into the ER by TAP, a subset bind to receptive H chain-β_2m heterodimers with high affinity, triggering dissociation of class I molecules from the PLC and their subsequent export from the ER to the cell surface (1, 2).

Although the functions of most of the participants in class I biogenesis are well understood, the details of how ERp57 functions in this process and its interplay with Cnx and Crt are less clear. ERp57 is one of at least 17 members of the mammalian protein-disulfide isomerase (PDI) family within the ER (3), and it catalyzes disulfide formation, isomerization, and reduction reactions *in vitro* through two C*XX*C active site motifs residing within thioredoxin-like domains (4, 5). Unlike other PDI family members that recognize substrates directly, ERp57 has been shown to require the presence of Cnx or Crt to promote disulfide bond formation in glycosylated substrates *in vitro* (6). Cnx and Crt recognize glycoprotein folding intermediates through a lectin site specific for $Glc_1Man_{5-9}GlcNAc_2$ oligosaccharides as well as through a polypeptide binding site that recognizes nonnative protein conformers (7, 8). Both sites reside within the globular lectin domain of Cnx and Crt, whereas the binding site for ERp57 resides at the tip of a second, extended arm domain (9–11). These sites are thought to act coordinately to bring ERp57 into the proximity of folding glycoproteins (6). In the case of class I molecules, ERp57 has been shown to promote

* This work was supported by Canadian Institutes of Health Research Grants MOP-53310 and MOP-74567 (to D. B. W. and K. G.) and a grant from the Canadian Cancer Society (to D. B. W.).

[1] To whom correspondence should be addressed: Dept. of Biochemistry, Medical Sciences Bldg., Rm. 5316, University of Toronto, Toronto, Ontario M5S 1A8, Canada. Tel.: 416-978-2546; Fax: 416-978-8548; E-mail: david.williams@utoronto.ca.

[2] The abbreviations used are: MHC, major histocompatibility complex; β_2m, β_2-microglobulin; Cnx, calnexin; Crt, calreticulin; CTL, cytotoxic T lymphocytes; DMEM, Dulbecco's modified Eagle's medium; DTT, dithiothreitol; ER, endoplasmic reticulum; H chain, heavy chain; mAb, monoclonal antibody; NEM, *N*-ethylmaleimide; PDI, protein-disulfide isomerase; PLC, peptide loading complex; siRNA, small interfering RNA; RNAi, RNA interference; HA, hemagglutinin; Ab, antibody; PBS, phosphate-buffered saline; MES, 4-morpholineethanesulfonic acid.

early H chain disulfide formation *in vivo*; depletion of ERp57 by RNA interference slowed the rate of formation of fully oxidized H chains by as much as 10-fold (12). However, a requirement for Cnx or Crt in this process was not examined, and it remains an open question whether these chaperones are essential for the full functionality of ERp57 in living cells, either for class I molecules or for other glycoprotein substrates.

ERp57 also functions at a later stage in class I biogenesis, at the level of the PLC. In addition to binding to Crt within the PLC, it forms a stable mixed disulfide conjugate with tapasin that involves Cys-57 of ERp57 and Cys-95 of tapasin (13). Garbi *et al.* (14) demonstrated that knock-out of ERp57 results in reduced stability of the PLC, lower surface expression of class I molecules, and decreased peptide presentation to CTL. Yet it remains unclear how ERp57 affects peptide loading of class I molecules within the PLC. It has been shown that mutagenesis of Cys-95 to Ala in tapasin to prevent formation of the ERp57-tapasin conjugate results in partially reduced class I H chains within the PLC (13). This has led to the suggestion that the reductase activity of ERp57 is restrained by tapasin so as to keep the class I H chain in a fully oxidized and peptide-receptive state within the PLC (15). Additional studies have suggested that ERp57 is solely a structural component that stabilizes the PLC (14) and that ERp57 in conjugation with tapasin edits peptide loading onto class I molecules, favoring high affinity peptides (16). It remains unclear whether ERp57 actually requires its enzymatic activity to function within the PLC, and the importance of its interaction with Crt within the PLC has not been established.

In this study, we take a mutagenesis approach, combined with RNAi, to examine the relationship between ERp57 and the lectin chaperones Cnx and Crt at early stages of oxidative H chain folding as well as during peptide loading in the PLC. We also examine the functions of active site mutants of ERp57 to assess the importance of its catalytic activities within the PLC. We show for the first time that ERp57 can catalyze H chain disulfide formation in the absence of interactions with Cnx and Crt and can also be recruited normally into the PLC. Thus, in living cells, ERp57 can gain access to H chains and tapasin without recruitment by lectin chaperones. Furthermore, catalytically inactive ERp57, lacking all active site cysteines except for Cys-57 that forms the conjugate with tapasin, was able to promote peptide loading in a manner similar to wild type ERp57. This suggests that ERp57 functions in a structural rather than a catalytic manner to assist tapasin in stabilizing the PLC and promoting the loading of optimal peptides onto class I molecules. Finally, we show that Crt can be incorporated into the PLC in the simultaneous absence of its lectin and ERp57-binding functions, illustrating the importance of polypeptide-based interactions in recognition of the class I substrate.

EXPERIMENTAL PROCEDURES

Cell Lines and Antibodies—Wild type ($ERp57^{+/+}$) and ERp57 knock-out ($ERp57^{-/-}$) mouse fibroblasts (14) were maintained in high glucose Dulbecco's modified Eagle's medium (DMEM; Sigma) supplemented with 10% fetal bovine serum, 2 mM L-glutamine, and antibiotics. Wild type (K41) and Crt knock-out (K42) mouse embryonic fibroblasts (17) as well as K42 cells transfected with various mutant Crt constructs were maintained in RPMI 1640 medium with fetal bovine serum, glutamine, and antibiotics. Mouse L cells stably expressing the class I molecules, H-$2K^b$ or H-$2D^d$, were cultured in DMEM supplemented with fetal bovine serum, glutamine, and antibiotics.

Antibodies used in this study were as follows: anti-8, a rabbit polyclonal antiserum, which recognizes all conformational states of the K^b molecule (18); monoclonal antibody (mAb) 34-2-12S, which recognizes the folded α3 domain of D^d molecules with an intact disulfide bond (19, 20); and mAbs Y3 (21) and B22.249 R1 (22), which react with β_2m-associated H-$2K^b$ and H-$2D^b$, respectively. Rabbit antisera directed against murine tapasin (23), murine Crt (24), canine Cnx (25), and murine ERp57 (12) have been described previously. Anti-TAP1 antiserum was a kind gift from Dr. Y. Yang (Johnson & Johnson Pharmaceutical Research and Development, San Diego, CA). Mouse anti-Crt mAb (SPA-601) and rabbit anti-PDI polyclonal antibody (SPA-890) were purchased from Assay Designs (Ann Arbor, MI), and mAb directed against glyceraldehyde 3-phosphate dehydrogenase was purchased from Millipore Corp. (Bedford, MA) (MAB374).

cDNA Isolation and Mutagenesis—RNA was isolated from mouse C2C12 myoblast cells using the TRIzol reagent according to the manufacturer's protocol (Invitrogen). Following reverse transcription with oligo(dT) primer and Stratascript reverse transcriptase (Stratagene), ERp57 cDNA was amplified by PCR using the following primers: mE57 forward, 5′-CGCGGATCC-GCCATGCGCTTCAGCTGCCTAGC; mE57 reverse, 5′-TTCCTTTTTTGCGGCCGCTTAGAGGTCCTCTTGTGCCTTCTTCTTCTTCTTAGG. The resulting cDNA was inserted into the pcDNA 3.1/Hygro(+) vector (Invitrogen). With this plasmid as template, the QuikChange II^{TM} site-directed mutagenesis kit (Stratagene) was used to mutate ERp57 residues involved in Cnx or Crt binding and also residues in the -CGHC- active sites. The following primers were used to convert the indicated ERp57 residues to alanine (numbering includes signal sequence); mutagenic bases are shown in lowercase type: R282A, forward (5′-TCTAACTACTGGAGAAACgctGTCATGATGGTGGCAAAGAAATTCC) and reverse (5′-GGAATTTCTTTGCCACCATCATGACagcGTTTCTCCAGTAGTTAGA); K214A, forward (5′-CGTCCATTACATCTTGCTAACgcgTTTGAAGACAAAACTGTGGC) and reverse (5′-GCCACAGTTTTGTCTTCAAAcgcGTTAGCAAGATGTAATGGACG); C406A/C409A, forward (5′-TGAATTTTACGCCCCTTGGgctGGCCACgctAAGAATCTGGAACCCAAG) and reverse (5′-CTTGGGTTCCAGATTCTTagcGTGGCCagcCCAAGGGGCGTAAAATTA); C60A, forward (5′-CCCTGGTGTGGACATgccAAGAGGCTTGCCCC) and reverse (5′-GGGGCAAGCCTCTTggcATGTCCACACCAGGG). C60A/C406A/C409A was made using C60A primers and C406A/C409A as template.

Wild type and mutant ERp57 cDNAs were then amplified and subcloned into the retroviral vector pQCXIH (Clontech, Mountain View, CA) using the following primers, which also introduced the NotI and BamHI restriction sites (underlined): forward, 5′-CCGAGCGCGGCCGCGCCATGCGCTTCAGCTGCCTAGC; reverse, 5′-TCGAGCGGATCCTTAGAGGTC-

CTCTTGTGCCTTCTTCTTC. Three micrograms of each Moloney virus vector, pVPack-GP, pVPack-VSV-G (Stratagene, La Jolla, CA), and pQCXIH containing the desired ERp57 cDNA construct, were diluted in 625 μl of Opti-MEM I reduced serum medium (Invitrogen). The DNA mixture was mixed with 22.5 μl of Lipofectamine 2000 (Invitrogen) prediluted in 625 μl of Opti-MEM I and incubated for 20 min at room temperature. The HEK293 packaging cell line was seeded at 1.4×10^6 cells/T25 flask in complete DMEM 18 h before transfection. The medium was exchanged for 2.5 ml of fresh DMEM without antibiotics, and then the DNA-Lipofectamine 2000 complex was added. After 4 h of transfection, the medium was replaced with 4 ml of fresh medium. The virus supernatant was collected 48 h post-transfection and filtered through a 0.22-μm filter before infecting target cells. Target cells, 4×10^5 ERp57$^{-/-}$ mouse embryonic fibroblasts, were infected in T25 flasks using 4 ml of undiluted virus supernatant in combination with 8 μg/ml Polybrene (Sigma). After 48 h of infection, cells were selected with 300 μg/ml hygromycin B for 3 days and 500 μg/ml hygromycin B for the following days. After 10 days to 1 month under selection, wild type and mutant ERp57 expression levels were obtained that were comparable with that observed in ERp57$^{+/+}$ cells as assessed by immunoblotting with anti-ERp57 antiserum. ERp57$^{+/+}$ and ERp57$^{-/-}$ cells infected with virus containing an empty pQCXIH vector were used as control cell lines.

To generate the ΔTip2 mutant of mouse Crt that possesses a truncated arm domain (amino acids 223–286 deleted), an overlap extension PCR (26) was performed. In the first round of PCR, mouse Crt cDNA in pcDNA3.1 (24) was used as the template to amplify a 699-bp and a 419-bp DNA fragment with the primer pairs (mutagenic bases in lowercase type; restriction sites underlined) NotI-mCrt-forward (5′-ATATGCGGCCGC-GCCACCATGCTCCTTTCGGTGCCGCTCCTGCT and mCrt-tip2-reverse (5′-AGGTACCgccactgccTCGTTCATCC-CAGTCTTC) and mCrt-tip2-forward (5′-TGAACGAggcagtg-gcGGTACCTGGATACACCCAG) and BamHI-Crt-reverse (5′-ATATATGGATCCCTAGAGCTCATCCTTGGCTTGG-CCAGGGGATTCT), respectively. After purification, the synthesized DNA fragments were used in equimolar amounts as the template in a second PCR to amplify the complete construct using the primer pair NotI-mCrt-forward/BamHI-Crt-reverse. The mutagenic PCR primers introduced a GSG linker at the site of truncation. All final PCR products were digested with NotI and BamHI and ligated into the retroviral expression vector pQCXIH (Clontech). To generate the ERp57 binding-deficient mutant of mouse Crt (D258N), a modified QuikChange™ protocol was performed (27) using the primer pair mCrt-D258N-forward (5′-GAAGAGATGaatGGAGAGTGGGAACCAC) and mCrt-D258N-reverse (5′-CACTCTCCattCATCTCT-TCATCCCAGTC) with mouse Crt cDNA in pcDNA3.1 as the template. The resulting plasmid pcDNA3.1-mCrtD258N was used as a template in a standard PCR with the primer pair NotI-mCrt-forward and BamHI-mCrt-reverse to introduce NotI and BamHI restriction sites into the cDNA for subcloning into the retroviral expression vector pQCXIH. Stable cell lines expressing the Crt-ΔTip2 and Crt-D258N mutants were prepared by infecting Crt-deficient K42 cells with recombinant Moloney viruses packaged with the respective pQCXIH plasmids as described above. Stable transformants were selected in 100 μg/ml hygromycin B.

For the HAΔEB mutant, we used a template plasmid provided by Drs. Lars Ellgaard and Eva Frickel (University of Copenhagen) encoding Crt in which the EDWDEEMD sequence of the arm domain was substituted with the SWWKELMH sequence of *Saccharomyces cerevisiae* Cnx and which also incorporated an influenza hemagglutinin (HA) tag prior to the COOH-terminal KDEL sequence. The Crt insert was amplified by PCR using the primers 5′-CCACTCGA-GGCCACCATGCTCCTTTCGGTGCCG (forward) and 5′-GTTCGGTTCCTACTCGACATCCAATTGTGG (reverse), which introduced XhoI and HincII restriction sites, respectively. The PCR product was digested with XhoI and HincII, subcloned into the Moloney murine leukemia virus vector CMV-bipep-ΔNGFR (28), and transfected into Phoenix cells (ATCC, Manassas, VA) using Lipofectamine 2000 (Invitrogen) according to the manufacturer's instructions (1 μg of DNA). On day 3, the cell culture medium containing retroviral particles was used to transduce Crt-deficient K42 cells. Cells were then cloned by limiting dilution.

Protein Expression, Preparation, and Purification—The arm domain of mouse Crt (residues 206–278; numbering including signal sequence) of mouse Crt was cloned into the pET15b plasmid (Amersham Biosciences) with an NH_2-terminal His_6 tag and expressed in *Escherichia coli* BL21 (DE3) cells. For NMR experiments, the recombinant protein was labeled by growth of *E. coli* BL21 in M9 minimal medium with ^{15}N-labeled ammonium chloride as the sole source of nitrogen. Cells were harvested and broken in 50 mM HEPES (pH 7.4), 300 mM NaCl, 1 mM β-mercaptoethanol, 5% glycerol. The fusion protein was purified by affinity chromatography on Ni^{2+}-chelating Sepharose resin, and the tag was removed by overnight cleavage with thrombin, leaving a Gly-Ser-His-Met NH_2-terminal extension while dialyzing the protein into 20 mM Tris (pH 8.0). The cleaved protein was additionally purified using anion exchange chromatography with a gradient of 0–1.0 M NaCl and exchanged into NMR buffer (20 mM MES, 50 mM NaCl, pH 6.5) using a Centricon 3000 concentrator. cDNAs encoding wild type Crt, the D317A and ΔTip2 mutants, and the D258N mutant of the Crt arm domain (residues 206–305) were cloned into a modified pET15b vector with a tobacco etch virus cleavage site and purified similarly with the exception that the His tag was not cleaved prior to NMR experiments. The wild type and the R282A mutant of the *bb′* fragment of human ERp57 were expressed and purified as described earlier (29).

NMR Spectroscopy—NMR stock solutions contained 0.2–0.3 mM protein in 20 mM MES, 50 mM NaCl at pH 6.5. For NMR titrations, unlabeled *bb′* fragments of ERp57 were added to ^{15}N-labeled 0.2 mM wild type or the D258N mutant of Crt arm domain to a final molar ratio of 1:1. All NMR experiments were performed at 30 °C using a Bruker 600-MHz spectrometer equipped with a cryoprobe. NMR spectra were processed using XWINNMR and analyzed with XEASY (30).

RNA Interference and Transfection—Knockdown of mouse ERp57 by RNA interference was performed as described previously (12). Double-stranded small interfering RNA (siRNA)

corresponding to mouse Cnx DNA sequence AATGTGGTG-GTGCCTATGTGA was synthesized and annealed by Qiagen (Valencia, CA). Eighteen hours before transfection, 1×10^5 K41 cells were seeded into 35-mm plates. Cells were then incubated with 80 nM siRNA or control siRNA plus Oligofectamine transfection reagent (Invitrogen) according to the manufacturer's protocol for 4 days before analysis. For all RNA interference experiments, $\sim 1 \times 10^5$ siRNA-transfected cells were used to assess the efficiency of protein depletion by Western blot.

Western Blotting Analysis—Cells were solubilized in Nonidet P-40 lysis buffer consisting of PBS, 1% Nonidet P-40, 20 mM *N*-ethylmaleimide (NEM; Sigma), and protease inhibitors (60 μg/ml 2-aminoethyl-benzenesulfonylfluoride and 10 μg/ml each leupeptin, antipain, and pepstatin (BioShop, Burlington, Canada)). Following centrifugation at 10,000 $\times$ *g* to remove nuclei and cell debris, the supernatant fractions were separated by SDS-PAGE (10% gel) before transfer to Immobilon membrane (Millipore) in buffer containing 25 mM Tris and 0.7 M glycine. Membranes were probed with various rabbit antisera followed by horseradish peroxidase-conjugated goat anti-rabbit secondary antibody. Proteins were detected by enhanced chemiluminescence, films were scanned using an EPSON 1680 scanner, and individual bands were quantified with NIH Image software (National Institutes of Health). In all cases, background values obtained by quantifying a blank area of the film corresponding in size to that of the gel band of interest were subtracted.

Metabolic Radiolabeling and Immunoisolation—All pulse-chase radiolabeling experiments were conducted on 5×10^5 cells growing in 35-mm plates. Cells were starved for 30 min with Met-free RPMI 1640 and then radiolabeled for 2 min with 0.5 ml of medium containing 0.1 mCi of [^{35}S]Met (>1000 Ci/mmol; Amersham Biosciences). Cells were then washed with Met-free RPMI 1640 and chased for various periods in DMEM containing 1 mM Met and 500 μM cycloheximide. Cells were placed on ice and treated for 3 min with 20 mM NEM in ice-cold PBS, pH 6.8, to minimize disulfide bond rearrangements. Lysis was conducted in 500 μl of Nonidet P-40 lysis buffer, and following centrifugation at 10,000 $\times$ *g*, the supernatant fraction was incubated on ice for 2 h with anti-8 antiserum or mAb 34-2-12S to isolate H-2K^b or H-2D^d, respectively. Immune complexes were recovered by shaking for 1 h with 30 μl of packed protein A-agarose beads. The beads were washed four times in 10 mM Tris, 0.5% Nonidet P-40, 150 mM NaCl, 0.02% NaN_3, pH 7.4, and then isolated molecules were eluted by boiling for 5 min in SDS-PAGE sample buffer with or without dithiothreitol (DTT) as a reducing agent. Samples were analyzed by SDS-PAGE (10% gel) followed by fluorography. Films were scanned, and protein bands were quantified as described above.

To test for interaction between Crt and various ERp57 constructs, 1×10^7 nonradiolabeled cells were collected and washed once with PBS before lysing the cells in digitonin lysis buffer (PBS containing 1% digitonin, 20 mM NEM, and protease inhibitor mixture). Crt was purified from postnuclear lysates using protein G beads precoated with mouse anti-Crt mAb. Samples were washed twice in PBS containing 0.2% digitonin, and isolated molecules were separated on SDS-PAGE and transferred to Immobilon membranes (Millipore) for immunoblotting with anti-ERp57 Ab. To examine the composition of the PLC, anti-tapasin antiserum, which was raised against a peptide corresponding to the carboxyl-terminal 20 amino acids of murine tapasin, was used to immunoisolate the PLC from digitonin cell lysates. Following collection of immune complexes on protein A-agarose, the PLC was eluted using a 100 μM concentration of the tapasin carboxyl-terminal peptide. This minimized elution of rabbit immunoglobulins from the beads, which would be detected in subsequent immunoblotting steps employing rabbit antisera directed against PLC components.

Flow Cytometry—To determine the cell surface levels of class I molecules, $3–5 \times 10^5$ cells were removed from culture plates by trypsinization and incubated on ice for 20 min in 100 μl of culture medium containing 1.5 μg of either mAb Y3 for K^b or mAb B22.249 R1 for D^b. After incubation, cells were washed once with fluorescence-activated cell sorting buffer (Hanks' balanced salt solution, 1% bovine serum albumin, and 0.01% NaN_3) and then incubated on ice for 20 min with 0.4 μg of phycoerythrin-conjugated goat anti-mouse IgG (H + L chain-specific; Cedarlane, Burlington, Canada) in 100 μl of fluorescence-activated cell sorting buffer. Cells were washed twice with fluorescence-activated cell sorting buffer and then fixed in 0.5% paraformaldehyde in PBS, pH 7.4. Subsequent flow cytometry was performed using a BD FACSCalibur Flow Cytometer (BD Biosciences).

Circular Dichroism Measurements—Wild type Crt and the D317A and ΔTip2 mutant proteins (10 μM) were incubated for 1 h at room temperature in 150 μl of 20 mM Hepes, pH 7.4, 150 mM NaCl, 1 mM $CaCl_2$ in the presence or absence of 100 μM Glcα3Manα2Manα2Man-OH oligosaccharide (Alberta Research Council, Edmonton, Alberta). Thermal denaturation was measured in a 1-mm path length cuvette by recording the change in ellipticity at 228 nm in the temperature range 26–60 °C with a scan rate of 2 °C/min using a Jasco 810 spectropolarimeter.

The recorded ellipticities were normalized to obtain the mean residue molar ellipticity ($[\Theta](\lambda)$) in degrees/cm^2/dmol according to the equation,

$$[\Theta](\lambda) = 100\frac{\Theta(\lambda)}{c \cdot n \cdot l} \qquad \text{(Eq. 1)}$$

where l represents the path length of the cuvette in centimeters, $\Theta(\lambda)$ is the recorded ellipticity in degrees at wavelength λ, c is the concentration in mol/liter, and n is the number of amino acid residues (422 for wild type Crt and D317A Crt and 361 for ΔTip2 Crt). Three independent denaturation curves were averaged under each condition. To determine T_m values (transition midpoint temperature of thermal unfolding), the measured averaged thermal denaturation curves were fit to a standard equation describing a two-state transition process by nonlinear least squares regression using SigmaPlot.

RESULTS

Expression of ERp57 Mutants and Their Interactions with Crt—We created several mutants of murine ERp57 to address the following two questions relating to its mechanism of action

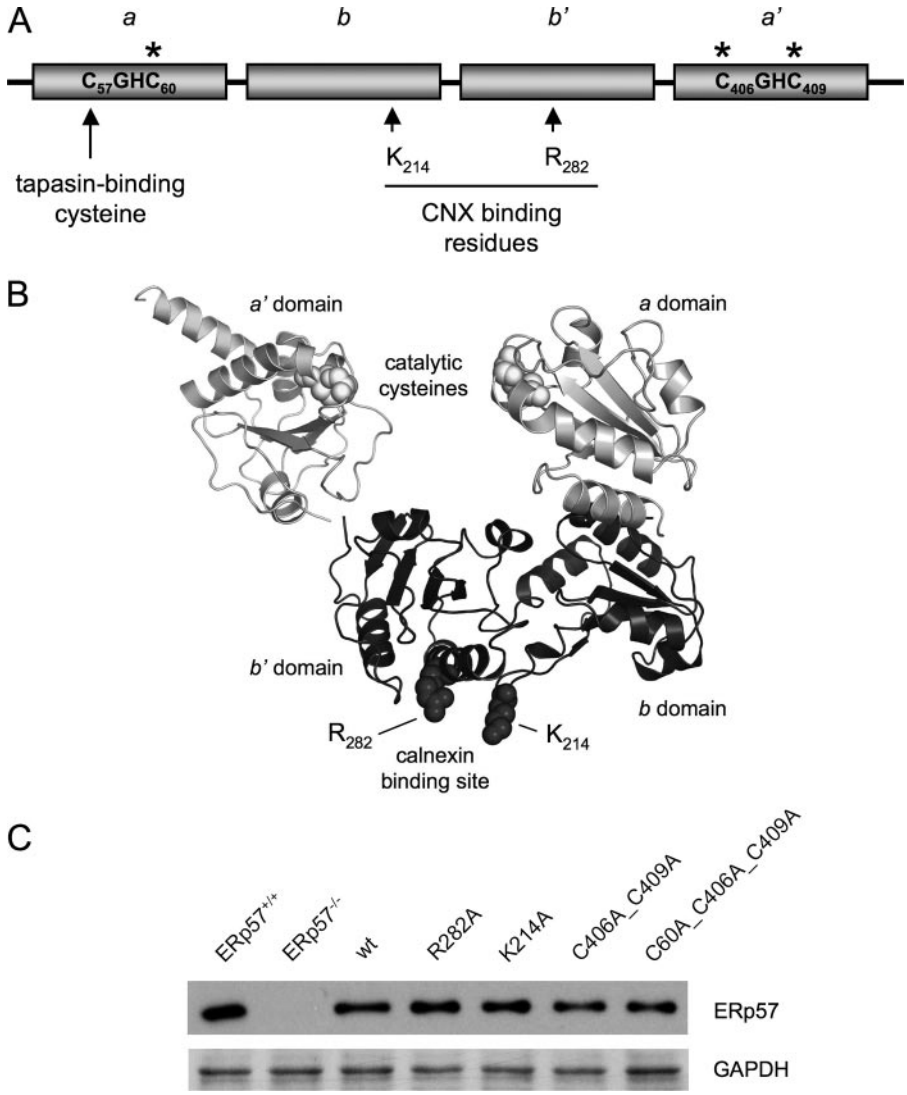

FIGURE 1. **Expression of wild type and mutant ERp57 in ERp57-deficient cells.** *A*, locations of mutated residues along the linear sequence of ERp57. Four thioredoxin-like domains (*a, b, b′*, and *a′*) are represented by rectangles with the active site sequence (CGHC) shown for the catalytic domains. Tapasin forms a disulfide bridge with ERp57 at cysteine 57. Cnx binding residues, Lys-214 and Arg-282, are shown in the noncatalytic *b* and *b′* domains. Active site cysteines that were mutated to alanines are marked with *asterisks*. *B*, locations of mutated residues within a three-dimensional representation of ERp57 constructed from the *a* and *a′* domains of PDI (37) and the *b* and *b′* domains of ERp57 (29). *C*, expression levels of wild type and mutant ERp57. ERp57-deficient mouse fibroblasts were infected with virus encoding wild type ERp57 (*wt*), Cnx-binding deficient ERp57 (*R282A* and *K214A*), and active site mutants of ERp57 (*C406A_C409A* and *C60A_C406A_C409A*). In addition, cells indicated as *ERp57*$^{+/+}$ and *ERp57*$^{-/-}$ were infected with virus packaged with an empty expression vector. After selection of stable transfectants in hygromycin B for 10 days, cells were lysed, and ERp57 was detected by immunoblotting. Lysates were also immunoblotted with anti-glyceraldehyde 3-phosphate dehydrogenase (*GAPDH*) antibody to serve as a loading control.

during class I biogenesis. 1) Are Cnx and Crt required to recruit ERp57 to class I H chains during early oxidative folding and subsequent peptide loading? 2) Is the catalytic activity of ERp57 essential for promoting peptide loading of class I molecules within the PLC? Concerning the first question, two residues were targeted, Arg-282 and Lys-214, with the intent of preparing ERp57 mutants that were incapable of binding to either Cnx or Crt. Previous studies have shown that mutation to alanine of Arg-282 (R282A) on the surface of the *b′* domain of ERp57 or of Lys-214 (K214A) on the β4-β5 loop of the *b* domain (Fig. 1, *A* and *B*) results in complete abrogation of Cnx binding or an 8-fold reduction in binding affinity, respectively (29). However, interaction of these mutants with Crt was not examined. For the second question, we disabled the catalytic activity of ERp57 in the *a′* domain by substituting the two cysteines in the active site with alanines (C406A/C409A). In addition, cysteine at position 60 in the *a* domain active site was replaced by alanine to selectively disable the oxidative activity of this domain (C60A/C406A/C409A). In both cases, we retained cysteine 57 in the *a* domain, which forms the stable, mixed disulfide linkage with tapasin.

The various ERp57 mutants were stably expressed along with wild type ERp57 in ERp57-deficient mouse fibroblasts using a Moloney virus expression system. To act as a control for any effects of the virus, ERp57$^{+/+}$ and ERp57$^{-/-}$ cells were also infected in the same manner with virus that was packaged with an empty expression vector. As shown in Fig. 1*C*, the expression levels of wild type and mutant ERp57 in the transfectants were comparable and resembled that observed in ERp57$^{+/+}$ cells.

To test whether the R282A and K214A mutants are as impaired in their ability to bind to Crt as they are to Cnx, transfected cells were lysed in digitonin lysis buffer, and Crt-ERp57 complexes were recovered by immunoisolation with anti-Crt antibody. The co-isolated ERp57 was detected by immunoblotting with anti-ERp57 antiserum (Fig. 2*A*). As expected, Crt-associated ERp57 was recovered from ERp57$^{+/+}$ cells as well as from ERp57$^{-/-}$ cells transfected with wild type ERp57. No ERp57 was recovered from Erp57$^{-/-}$ cells, and only a trace amount was recovered from Crt-deficient K42 cells, indicating the specificity of the immunoisolation procedure. Mutation of Arg-282 to alanine dramatically diminished the interaction of ERp57 with Crt, whereas the K214A mutant was only modestly impaired, exhibiting 60% binding relative to wild type ERp57 (Fig. 2*A*). To confirm that R282A does not interact with Crt, we performed NMR experiments in which unlabeled *bb′* fragments of wild type or R282A ERp57 were added at a 1:1 molar ratio to the ^{15}N-labeled Crt arm domain (Fig. 2*B*). In these ^{1}H-^{15}N HSQC spectra, signals arising from the free Crt arm domain are in *cyan*, and, after adding ERp57 *bb′* domains, the signals are

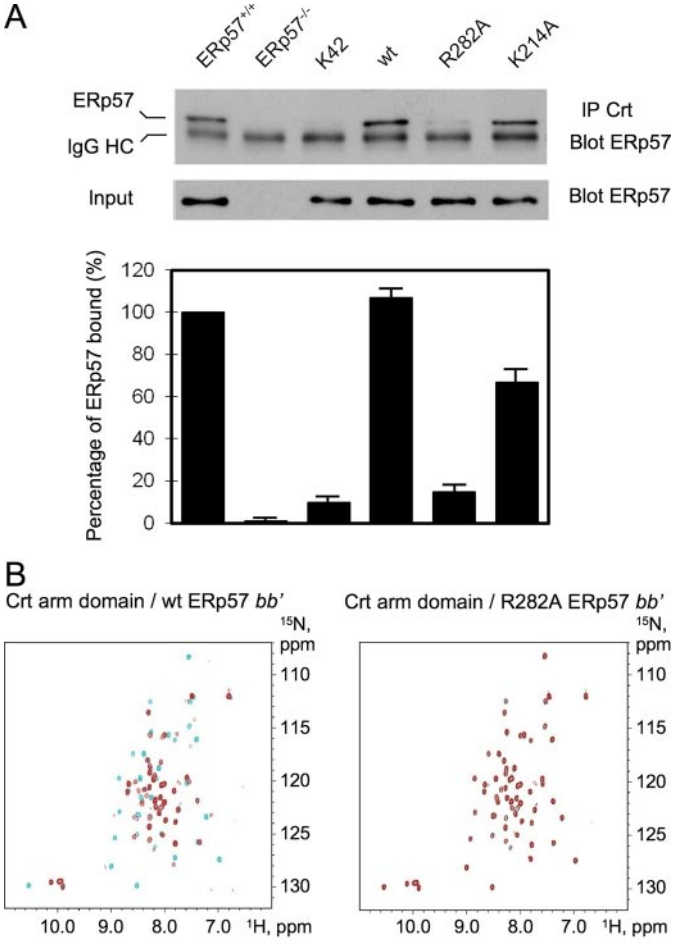

FIGURE 2. **Interaction of ERp57 mutants with Crt.** *A*, the indicated cell lines were lysed in 1% digitonin lysis buffer and then subjected to immunoisolation with mouse anti-Crt antibody. Immune complexes were resolved by SDS-PAGE, and co-isolated ERp57 was identified by immunoblotting with rabbit anti-ERp57 antiserum. Separate aliquots of lysates from equal numbers of cells were also immunoblotted to serve as loading inputs. Results were quantified by densitometry and are shown as a percentage of ERp57 bound to Crt in parental ERp57$^{+/+}$ cells. The values are the averages of three replicate experiments, with *error bars* representing S.E. *B*, assessment of interaction between Crt and wild type or R282A ERp57 by NMR spectroscopy. Shown are HSQC spectra of the ^{15}N-labeled wild type Crt arm domain (residues 206–278) acquired in the absence (*cyan*) and presence (*red*) of the *bb'* fragment of either wild type ERp57 (*left*) or the R282A mutant (*right*). *wt*, wild type; *IP*, immunoprecipitation.

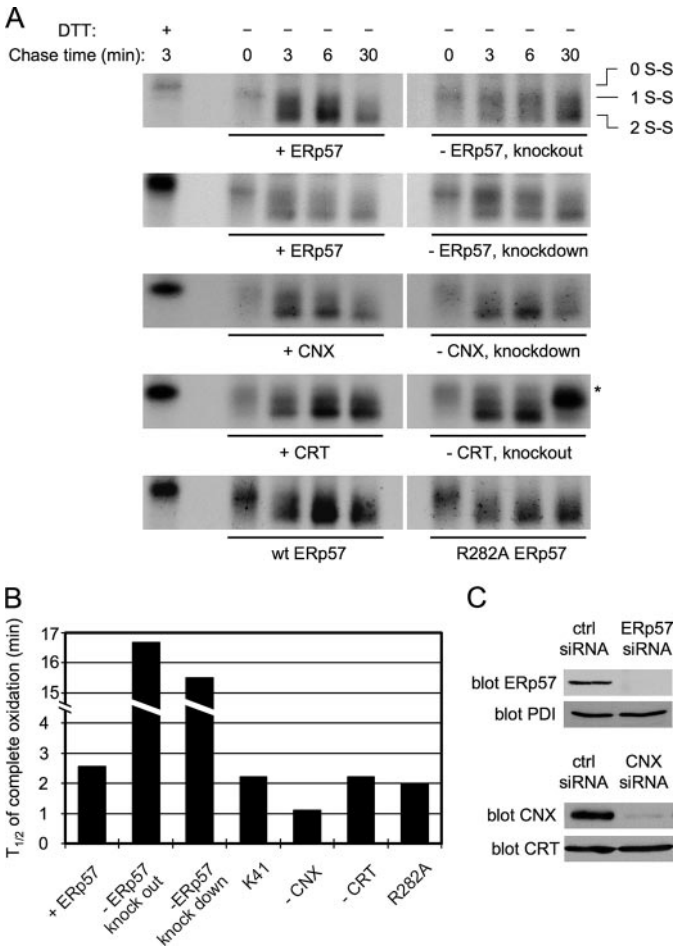

FIGURE 3. **The catalytic activity of ERp57 toward class I H chains is independent of interactions with Cnx and Crt.** *A*, kinetics of K^b H chain disulfide bond formation were measured in ERp57 knock-out cells (*first gel*), K^b-expressing L cells depleted of ERp57 by RNAi (*second gel*), K41 cells depleted of Cnx by RNAi (*third gel*), K42 Crt knock-out cells (*fourth gel*), and ERp57 knock-out cells expressing the R282A mutant of ERp57, which does not bind Cnx or Crt (*fifth gel*). In all cases, the wild type (*wt*) condition is depicted on the *left half* of each gel. Cells were radiolabeled for 2 min with [^{35}S]Met and chased with unlabeled medium containing cycloheximide for the indicated periods. Cells were then incubated in cold PBS, pH 6.8, containing 20 mM NEM to prevent disulfide rearrangement and subsequently lysed in buffer containing NEM. K^b H chain was immunoisolated with anti-8 antiserum and separated by nonreducing SDS-PAGE. H chains containing different numbers of disulfide bonds are indicated by *0*, *1*, and *2 S-S*. The *leftmost* sample on each gel was treated with DTT to provide a mobility standard of fully reduced K^b H chain (*0 S-S*). *, nonspecifically recovered band in immunoisolates from K41 and K42 cells. *B*, the rate of disulfide bond formation was measured as the time at which 50% of H chains were fully oxidized ($t_{1/2}$). Fluorograms were scanned, and bands corresponding to H chains with one or two disulfides were selected by boxes of equal size and quantified using NIH Image software. Following background subtraction, the percentage of fully oxidized species at each time point was calculated and plotted. $t_{1/2}$ values were measured from the *graphs* and are depicted as *histograms*. Data are representative of 2–3 independent experiments per cell line. *C*, extent of knockdown of ERp57 and Cnx following siRNA treatment. Equivalent numbers of cells treated with control or either ERp57 or Cnx siRNA were lysed, loaded on an SDS-polyacrylamide gel, and immunoblotted with anti-ERp57 or anti-Cnx Abs. The blots were reprobed with anti-PDI or anti-Crt antibodies to serve as loading controls (*ctrl*) and to demonstrate the specificity of knockdown.

marked in *red*. When the Crt arm domain and wild type ERp57 *bb'* domain were examined, there were many shifted signals indicative of interaction (Fig. 2*B*, *left*). However, the spectra were superimposable in the case of the R282A mutant, demonstrating that binding to Crt was completely abolished when Arg-282 of ERp57 was mutated to alanine.

ERp57 Catalyzes H Chain Disulfide Formation in the Absence of Interactions with Cnx and Crt—We showed previously that in living cells, the rate at which MHC class I H chains acquire a fully oxidized set of disulfide bonds is markedly reduced upon depletion of ERp57 by RNAi (12). This was confirmed in the present study by using ERp57 knock-out mouse fibroblasts (Fig. 3). Wild type and ERp57 knock-out cells were radiolabeled for 2 min with [^{35}S]Met and chased for periods of up to 30 min. H-2K^b molecules were recovered from cell lysates and analyzed by SDS-PAGE under nonreducing conditions to allow resolution of species containing zero, one, or two disulfide bonds (Fig. 3*A*, *top*; quantified in Fig. 3*B*). As observed previously in ERp57-positive cells, the first H chain disulfide formed very rapidly, possibly co-translationally, during the 2-min pulse; hence, no H chains with zero disulfide bonds were detected. The second

disulfide formed more slowly, with 50% of H chains acquiring both disulfide bonds by 2.5 min of chase. By contrast, in ERp57 knock-out cells, the first disulfide formed normally, but the rate at which H chains acquired the second disulfide was ~7-fold slower, with a half-time exceeding 15 min. This dependence of H chain disulfide formation on ERp57 was also observed when ERp57 expression was reduced by more than 90% through RNAi (Fig. 3, *A* (*second gel*) and *C*), consistent with previous results (12). The half-time of formation of the second disulfide was slowed from 2.5 min to ~15 min (Fig. 3*B*).

To assess the role of Cnx and Crt in recruiting ERp57 to H chains during oxidative folding, we initially examined H chain disulfide formation in cells deficient in or depleted of the chaperones. We reasoned that if either of these chaperones is required to recruit ERp57 to H chains, loss of the chaperone should result in a slow H chain oxidation phenotype similar to ERp57 deficiency. RNAi was used to knock down Cnx expression in mouse K41 embryonic fibroblasts that express class I K^b molecules. After transfection with Cnx siRNA or with control siRNA, greater than 90% of Cnx was depleted after 4 days with no impact on Crt expression (Fig. 3*C*). Disulfide bond formation in K^b H chains was then monitored in a pulse-chase experiment, as described above. The results showed that disulfide bond formation was not affected by the depletion of Cnx, with most H chains fully oxidized after 3–6 min of chase (Fig. 3*A*, *third gel*; quantified in Fig. 3*B*). A similar experiment was performed comparing Crt knock-out embryonic fibroblasts (K42 cells) with wild type K41 cells, both of which express K^b molecules endogenously. As shown in the *fourth gel* of Fig. 3*A*, H chain disulfide bonds formed at similar rates in the presence or absence of Crt, indicating that Crt, like Cnx, was not required for ERp57 to catalyze H chain disulfide formation. Note that in the absence of Crt, K^b molecules were exported faster from the ER, resulting in slower electrophoretic ability at the 30 min time point as processing of its oligosaccharide chains occurred (Fig. 3*A*, *fourth gel*). This phenomenon has been documented previously (31). To exclude the possibility that depletion of only one of the chaperones permits compensation by the other, we made use of the ERp57 mutant R282A, which does not interact with either Cnx or Crt. Upon expressing the R282A mutant in $ERp57^{-/-}$ cells, we found that the slow disulfide bond formation phenotype in $ERp57^{-/-}$ cells was fully complemented by the R282A mutant (Fig. 3*A*, *fifth gel*). Although the $t_{1/2}$ for complete oxidation of K^b H chains was greater than 15 min in ERp57-deficient cells, this was reduced to ~2 min in the R282A transfectant, a rate similar to that of wild type cells. These observations indicate that ERp57 does not need to be recruited by Cnx or Crt to catalyze disulfide formation in MHC class I molecules.

Since Cnx is the predominant chaperone that interacts with class I H chains during early disulfide formation, we sought an independent means to assess the involvement of Cnx in ERp57-catalyzed H chain oxidation. mAb 34-2-12S only recognizes class I D^d molecules that have acquired a disulfide bond within their membrane-proximal α3 domain (20), and we have shown previously that it is the formation of this disulfide that is slowed upon ERp57 depletion (12). Consequently, we used RNAi to deplete either ERp57 or Cnx by more than 90% from L cells

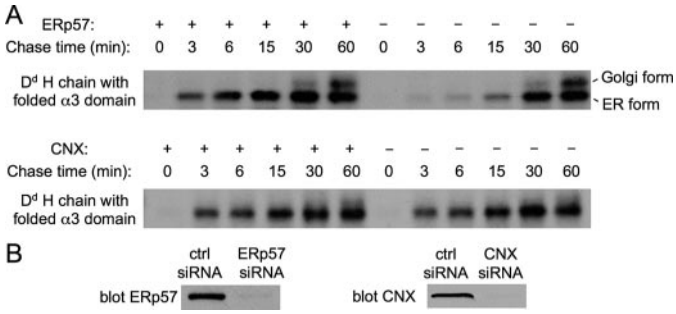

FIGURE 4. **Slower D^d α3 domain folding occurs upon depleting ERp57 but not Cnx.** *A*, kinetics of D^d α3 domain folding examined by pulse-chase radiolabeling. After depleting ERp57 (*top gel*) or Cnx (*bottom gel*) by RNAi, L cells expressing D^d molecules were radiolabeled with [^{35}S]Met for 2 min and chased with unlabeled medium containing cycloheximide for various periods. Cells were washed in ice-cold PBS (pH 6.8) containing NEM (20 mM) for 3 min and lysed in 1% Nonidet P-40 lysis buffer with NEM. D^d H chains with a disulfide-bonded α3 domain were recovered from postnuclear lysates with mAb 34-2-12S and analyzed by reducing SDS-PAGE. *B*, the extent of target protein knockdown by RNA interference. Equivalent numbers of cells treated with control (*ctrl*), ERp57, or Cnx siRNA were lysed, loaded on an SDS-polyacrylamide gel, and immunoblotted with either anti-ERp57 or anti-Cnx Abs.

expressing D^d molecules (Fig. 4*B*) and then monitored the kinetics of mAb 34-2-12S epitope formation in a pulse-chase radiolabeling experiment. In both cases, a set of cells was treated with control siRNA and underwent the same procedures. As shown in Fig. 4*A* (*top*), the α3 domain disulfide formed more slowly when ERp57 expression was reduced by RNAi compared with cells treated with control siRNA. In contrast, depletion of Cnx had no such effect (Fig. 4*A*, *bottom*). This result reinforces the conclusion that Cnx is dispensable for the functionality of ERp57 toward class I H chains.

ERp57 That Fails to Bind Cnx and Crt or That Lacks Catalytic Activity Is Functional within the PLC—We next explored the characteristics of ERp57 that contribute to its functions in stabilizing the PLC and in promoting peptide loading of class I molecules. ERp57 exists within the PLC as a stable, disulfide-linked conjugate between cysteine 57 of ERp57 and cysteine 95 of tapasin; mutation at either residue abolishes conjugate formation (13). To test the importance of ERp57 interactions with Cnx and/or Crt for its recruitment into conjugates with tapasin, we used the ERp57 mutants that either do not bind Cnx and Crt (R282A) or have reduced binding affinity (K214A). Both mutants were expressed in $ERp57^{-/-}$ cells, and, after treating cells with NEM, lysates were separated by nonreducing SDS-PAGE and immunoblotted with anti-tapasin antiserum or anti-ERp57 antiserum to detect ERp57-tapasin conjugates (Fig. 5). Both R282A and K214A were capable of forming disulfide-linked conjugates with tapasin, as shown by the immunoreactive band at 110 kDa. This band was confirmed to be the ERp57-tapasin conjugate on the basis of its immunoreactivity with both antisera, its disappearance upon reduction with DTT, and its absence in $ERp57^{-/-}$ cells. These findings indicate that interactions with Cnx and/or Crt are not required to recruit ERp57 into the PLC for conjugate formation with tapasin.

To test whether the ERp57 mutants that either lack or are impaired in lectin chaperone binding remain functional within the PLC, we examined their abilities to stabilize peptide-receptive class I molecules within the PLC and promote peptide loading. It has been shown previously that although PLCs form in

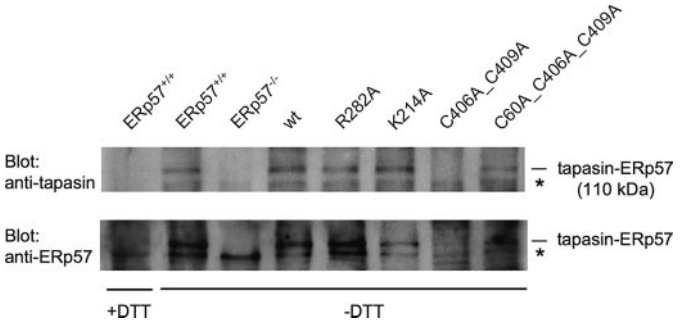

FIGURE 5. **Conjugate formation between tapasin and ERp57 mutants.** Mouse fibroblasts expressing ERp57 mutants were incubated in cold PBS, pH 6.8, containing 20 mM NEM to prevent disulfide rearrangement and subsequently lysed in 1% Nonidet P-40 lysis buffer containing NEM. The post-nuclear cell lysates were subjected to nonreducing SDS-PAGE and immunoblotted with either anti-tapasin (*top gel*) or anti-ERp57 (*bottom gel*) Abs. The samples in the *leftmost lanes* of both gels were treated with DTT before loading. *, nonspecific band that was detected at various levels in all samples, including those lacking ERp57. *wt*, wild type.

the absence of functional ERp57, they are unstable, and bound class I molecules dissociate rapidly (14). We isolated PLCs using anti-tapasin antiserum and tested for the presence of associated peptide-receptive K^b molecules by immunoblotting. As shown in Fig. 6*A*, K^b molecules could be recovered readily from PLCs of $ERp57^{+/+}$ cells (*lane 4*) or of $ERp57^{-/-}$ cells transfected with wild type ERp57 (*lane 6*), but they were present in only trace amounts in PLCs from $ERp57^{-/-}$ cells (*lane 5*). K^b molecules could also be recovered from $ERp57^{-/-}$ cells expressing the R282A and K214A mutants of ERp57 (*lanes 7* and *8*), indicating that despite absent or impaired interactions, respectively, with Cnx and Crt, ERp57 remains capable of stabilizing the PLC. The ability of ERp57 to promote peptide loading of class I molecules has been demonstrated directly by monitoring the creation of specific peptide-class I complexes (14) as well as indirectly by measuring the levels of total cellular class I molecules by immunoblotting (15) or the levels of surface class I molecules by flow cytometry (24). Peptide-receptive class I molecules are unstable relative to those containing high affinity peptides, which leads to reduced cell surface or total levels when peptide loading is impaired. Fig. 6*B* shows that the level of total cellular K^b molecules in $ERp57^{-/-}$ cells was about 35% of that observed in $ERp57^{+/+}$ cells or in $ERp57^{-/-}$ cells expressing wild type ERp57. Both the R282A and K214A mutants of ERp57 were capable of promoting peptide loading of K^b molecules and stabilizing them to an extent similar to wild type ERp57. A similar result was obtained when surface K^b expression was measured (Fig. 7*A*). The K214A mutant was just as effective as wild type ERp57 in normalizing the low surface expression phenotype observed in $ERp57^{-/-}$ cells. The R282A mutant was slightly less effective, restoring surface K^b levels to about 85% of that observed in wild type cells or $ERp57^{-/-}$ cells expressing wild type ERp57. When D^b expression was examined, the K214A mutant fully complemented the low surface expression observed in $ERp57^{-/-}$ cells, but the R282A mutant was clearly less effective, restoring surface levels to about 60% of control. These results suggest that although interactions with Cnx and Crt are not needed for the formation of ERp57-tapasin conjugates and for stabilizing class I molecules within the PLC, chaperone interactions with ERp57 appear to have a significant

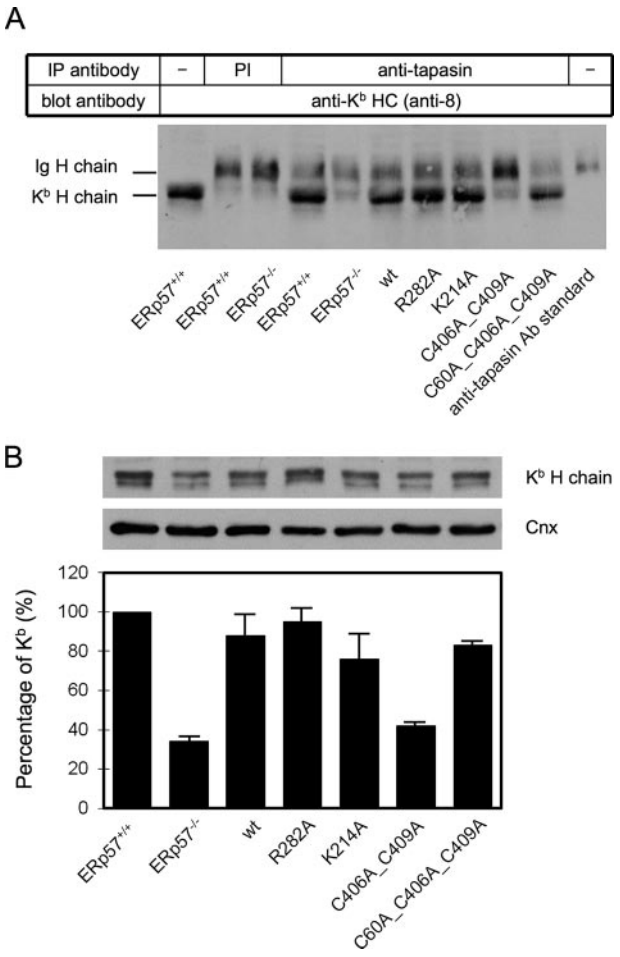

FIGURE 6. **Detection of class I molecules in peptide loading complexes and in lysates from cells expressing ERp57 mutants.** *A*, cells expressing the indicated ERp57 mutants were lysed in digitonin lysis buffer and then subjected to immunoisolation with either preimmune serum (*PI*) or anti-tapasin antiserum. Immune complexes recovered with protein A-agarose were dissociated with a 100 μM concentration of the COOH-terminal tapasin peptide used to raise the antiserum, and released proteins were separated by SDS-PAGE and immunoblotted with anti-8 antiserum to detect K^b molecules. Note that a small amount of Ig heavy chain (50 kDa) was released from the protein A beads during the elution step and migrated just above the K^b H chain (45 kDa). *B*, the steady-state levels of K^b molecules were detected by immunoblotting cell lysates using anti-8 antiserum. H chain bands were quantified by densitometry and plotted as a percentage of the amount present in $ERp57^{+/+}$ cells. In the *lower gel*, cell lysates were immunoblotted with anti-Cnx antiserum to serve as a loading control. *Error bars* represent S.E. based on three independent experiments. *IP*, immunoprecipitation; *wt*, wild type.

impact on the efficiency of peptide loading, particularly for D^b molecules.

It remains unclear whether the catalytic activity of ERp57 is important for its functions within the PLC (16). To address this issue, we examined two mutants of ERp57 that affected catalytic activity while preserving Cys-57 to permit conjugate formation with tapasin. In the first mutant, both active site cysteines in the *a′* domain were mutated to alanine, thereby inactivating this domain (C406A/C409A). As shown in Fig. 5, the C406A/C409A mutant could not be detected in a disulfide-linked conjugate with tapasin. This has been observed previously (13) and suggests some degree of cooperativity between the two C*XXC* active sites. In the second mutant, the cysteine at position 60 was mutated to alanine in addition to the mutations at Cys-406 and Cys-409, which fully disables enzymatic activity.

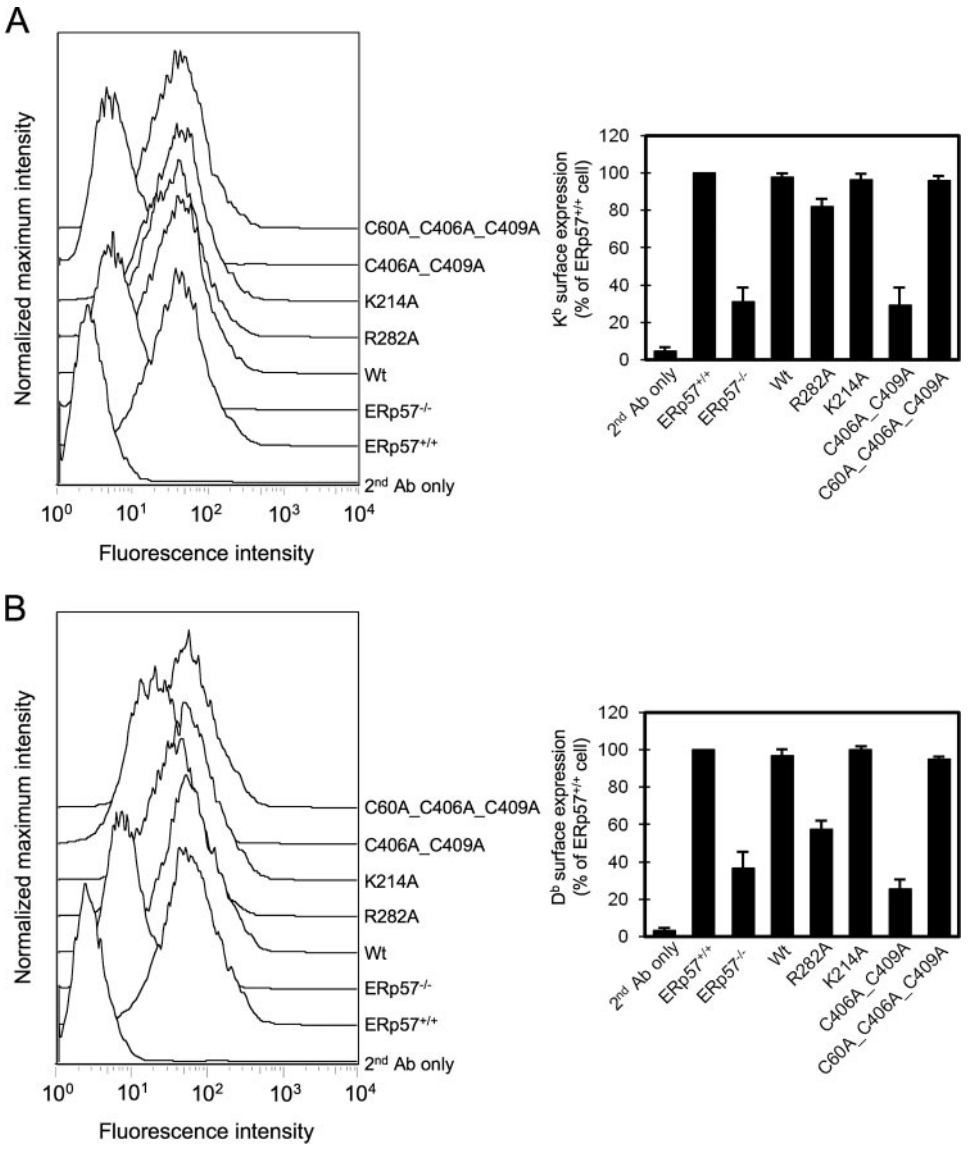

FIGURE 7. **Effect of ERp57 mutations on cell surface expression of MHC class I molecules.** *A*, cell surface expression of K^b molecules detected by flow cytometry. ERp57$^{-/-}$ cells expressing the indicated wild type or mutant ERp57 molecules were incubated with mAb Y3, followed by incubation with phycoerythrin-conjugated goat anti-mouse IgG and analysis by flow cytometry. The mean fluorescence obtained for each mutant was plotted relative to that of ERp57$^{+/+}$ cells, which was set to 100%. *Error bars* represent S.E. values based on three independent experiments. *B*, cell surface expression levels of D^b molecules detected by flow cytometry. The method was the same as in *A*, except mAb B22.249R1 was used as the primary antibody to detect D^b molecules. *Wt*, wild type.

Interestingly, this triple mutant (C60A/C406A/C409A) could be detected as a mixed disulfide with tapasin, albeit at a reduced level compared with wild type ERp57 (Fig. 5). The detection of the conjugate in the triple mutant as opposed to the double mutant is probably due to a stabilization of the conjugate through inactivation of an "escape pathway" mediated by Cys-60. In this pathway, a mixed disulfide formed by the NH_2-terminal Cys of a C*XX*C motif, such as the conjugate with tapasin, is resolved through attack by the COOH-terminal Cys of the motif (32).

We next examined the abilities of the active site mutants to stabilize the PLC and promote peptide loading of class I molecules. As shown in Fig. 6*A* (*lane 10*), the C60A/C406A/C409A mutant, which formed a conjugate with tapasin, was capable of stabilizing peptide-receptive K^b molecules within the PLC, albeit at a somewhat reduced level compared with wild type cells. In contrast, the C406A/C409A mutant, which was unable to form a conjugate with tapasin, lacked the ability to stabilize class I molecules within the PLC, resembling ERp57$^{-/-}$ cells (compare *lanes 5* and *9*). This double mutant also failed to promote peptide loading and exhibited the same low level of total cellular K^b molecules (Fig. 6*B*) and reduced surface expression of K^b and D^b molecules as observed in ERp57$^{-/-}$ cells (Fig. 7). Remarkably, the C60A/C406A/C409A triple mutant was just as effective as wild type ERp57 in promoting efficient peptide loading, as assessed by the stabilization of total cellular K^b molecules (Fig. 6*B*) and by restoring normal surface K^b and D^b expression to ERp57$^{-/-}$ cells (Fig. 7). This indicates that the thiol oxidoreductase activity of ERp57 is dispensable for PLC stabilization and peptide loading and suggests that ERp57 plays a structural as opposed to a catalytic role within the PLC.

Interactions between ERp57 and Crt Are Not Required for Crt Recruitment into the Peptide Loading Complex—The availability of the ERp57 R282A mutant also provided an opportunity to examine the factors that determine the incorporation of Crt into the PLC. Within the PLC, Crt associates noncovalently with the class I H chain through its lectin site (16, 33) and possibly its polypeptide binding site (24) and with ERp57 through the tip of its arm domain (9, 10). Our recent finding that lectin-deficient Crt could still be recruited into the PLC (24) raised the possibility that the interaction between Crt and ERp57 could play a significant role in stabilizing or incorporating Crt. Further support for this notion comes from the fact that Crt is dramatically reduced in the PLC isolated from ERp57 knock-out cells (14). To test the importance of the Crt-ERp57 interaction more directly, we used anti-tapasin antiserum to isolate the PLC from ERp57 knock-out cells expressing the Crt binding-deficient mutant of ERp57, R282A. The presence of Crt in the PLC was then detected by immunoblotting with anti-Crt antiserum. As shown in Fig. 8*A*, Crt was present in the PLC of wild type ERp57$^{+/+}$ cells and in ERp57 knock-out cells transfected with either wild type ERp57 or K214A mutant ERp57 (which

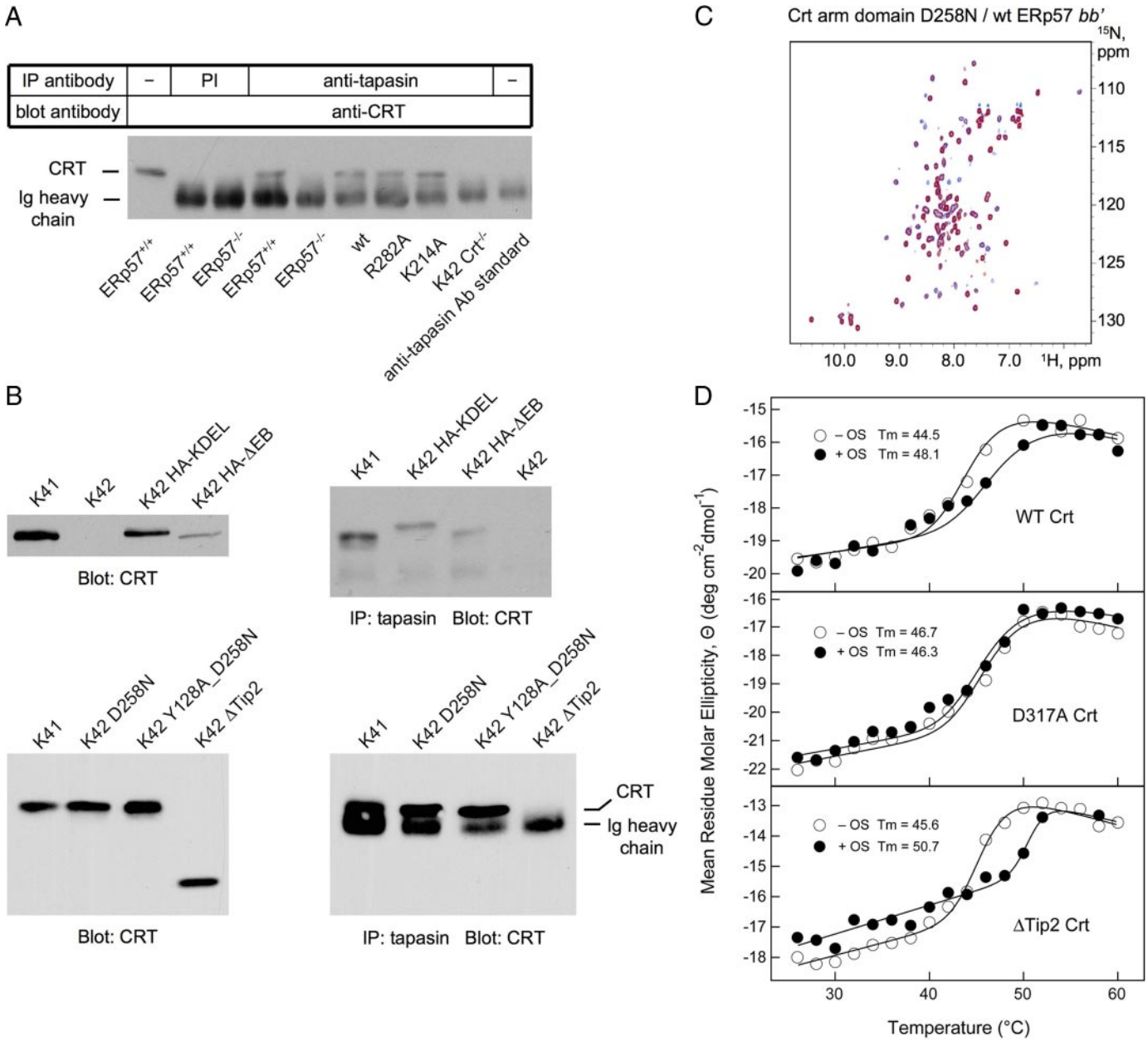

FIGURE 8. **Detection of Crt in the peptide loading complex of cells expressing mutant forms of ERp57 or Crt.** *A*, interaction with ERp57 is not required for recruitment of Crt into the PLC. The indicated cell lines were lysed in digitonin lysis buffer and then subjected to immunoisolation with either preimmune serum (*PI*) or anti-tapasin antiserum. Immune complexes were dissociated with a 100 μM concentration of the COOH-terminal tapasin peptide used to raise the antiserum, and released proteins were separated by SDS-PAGE and immunoblotted with anti-Crt antiserum. Some Ig heavy chains (50 kDa) were released during the dissociation procedure and migrate just below Crt (60 kDa). The absence of Crt in the lanes immunoisolated with preimmune serum and the lane using Crt-deficient K42 cells demonstrated the specificity of the immunoisolation procedure. *B*, Crt is recruited into the PLC independently of its lectin- and ERp57-binding functions. The indicated cell lines were lysed in Nonidet P-40 lysis buffer, and aliquots corresponding to equivalent numbers of cells were separated by SDS-PAGE and immunoblotted with anti-Crt antiserum (*left*). The presence of Crt in peptide loading complexes isolated from these cells was detected as described for *A* (*right*). *C*, the D258N mutant of Crt does not interact with ERp57. Shown are HSQC spectra of the ^{15}N-labeled D258N arm domain mutant of Crt (residues 206–305) acquired in the absence (*cyan*) and presence (*red*) of the wild type *bb'* fragment of ERp57. Except for several weak resonances arising from noise in each spectrum, the two patterns were superimposable, indicative of no binding. *D*, Crt with a truncated arm domain exhibits normal thermal stability and lectin function. Thermal denaturation curves of wild type Crt, lectin-deficient D317A Crt, and arm-truncated ΔTip2 Crt were obtained by heating from 26 to 60 °C and measuring changes in mean residue ellipticity by circular dichroism. The experiments were repeated in the presence of 100 μM Glcα3Manα2Manα2Man-OH oligosaccharide (*OS*), which, upon binding to Crt, results in stabilization of the protein, as detected by an increase in melting temperature (T_m). *IP*, immunoprecipitation; *wt*, wild type.

retains partial ability to interact with Crt; Fig. 2*A*) but not in mock-transfected ERp57$^{-/-}$ cells. Remarkably, in ERp57 knock-out cells expressing R282A ERp57, Crt was readily detected within the PLC despite the inability of this mutant to bind to the chaperone (Fig. 8*A*). These findings suggest that the interaction between Crt and ERp57 is not required for the stable incorporation of Crt into the PLC and that the absence of Crt in the PLC of ERp57 knock-out cells is a consequence of something more than the simple loss of binding to ERp57.

To confirm this finding, we performed additional experiments in which the Crt-ERp57 interaction was disrupted by mutating the tip of the Crt arm domain. This segment of the

arm domain of Crt and Cnx is highly conserved, with the exception of the *S. cerevisiae* homolog of Cnx, Cne1p, since this organism lacks ERp57 (34, 35). Ellgaard and co-workers[3] replaced the EDWDEEMD sequence of the mouse Crt arm domain with the SWWKELMH of Cne1p and also inserted an HA tag immediately upstream of the COOH-terminal KDEL sequence (HA-ΔEB). *In vitro* cross-linking studies and binding studies using isothermal titration calorimetry and enzyme-linked immunosorbent assays verified that the mutated Crt arm domain failed to bind ERp57.[3] HA-ΔEB and HA-KDEL (HA-tagged wild type Crt) were expressed in $Crt^{-/-}$ K42 cells using a retroviral vector, and expression was confirmed by immunoblot (Fig. 8*B*, *top left*). HA-ΔEB expression was lower than HA-KDEL, and the arm domain mutant exhibited slightly faster electrophoretic mobility, presumably due to the multiple substitutions of charged residues. The PLCs were immunoisolated with anti-tapasin Ab, and the presence of Crt in the PLC was determined by immunoblotting as above. As shown in Fig. 8*B* (*top right*), ERp57 binding-deficient Crt (HA-ΔEB) was readily detected in the PLC, confirming that the stable incorporation of Crt in the PLC does not require an interaction with ERp57.

Considering our previous finding that disruption of the Crt lectin site did not exclude it from the PLC (24) as well as the present observation that interaction with ERp57 is not required, it was of interest to construct a mutant Crt that does not interact with either ERp57 or oligosaccharide chains on glycoproteins and test for its presence in the PLC. During the course of this work, we found that mutation of a single residue at the tip of the Crt arm domain, Asp-258, was just as effective in abolishing the interaction with ERp57 as the extensive substitution of residues from *S. cerevisiae* Cne1p. As shown in the ^{1}H-^{15}N HSQC spectrum of Fig. 8*C*, the D258N mutant was unable to interact with the *bb′* domains of ERp57. We combined this mutation with Y128A, a point mutation within the lectin site of Crt that results in a complete loss of binding to $[^{3}H]Glc_1Man_9GlcNAc_2$ oligosaccharide but does not alter Crt structure, as determined by protease sensitivity and CD analysis (36). The D258N single mutant and Y128A/D258N double mutant were expressed in K42 cells (Fig. 8*B*, *bottom left*). The single mutant was detected in the PLC as expected, but surprisingly, the double mutant that lacks both ERp57 binding and lectin function was also strongly present in the PLC (Fig. 8*B*, *bottom right*). Since Crt is present within the PLC despite the lack of interaction with ERp57 and with oligosaccharides, an interaction through the Crt polypeptide binding (chaperone) site must be responsible.

The polypeptide binding site of Crt and Cnx is responsible for the ability of these chaperones to suppress the aggregation of nonnative proteins *in vitro*. Although this site has not been precisely mapped, it resides within the globular domain of these chaperones at a location distinct from the lectin site (57). Although the arm domain has no capacity to suppress aggregation on its own, its presence is required for the full aggregation suppression function mediated by the globular domain (57). We tested what the effect might be on Crt recruitment into the PLC if the two-thirds of the arm domain were removed. This ΔTip2 mutant would be expected to have intact lectin function, no capacity to bind ERp57, and an impaired ability to interact with nonnative polypeptides. Fig. 8*D* demonstrates that the ΔTip2 mutant remained properly folded, since it exhibited thermal stability similar to that of wild type Crt (T_m = 44.5 and 45.6 °C for Crt and ΔTip2, respectively; Fig. 8*D*). It also retained the ability to bind oligosaccharide, as evidenced by an increase in melting temperature (stability) upon the addition of oligosaccharide, compared with D317A Crt, which, like Y128A, is completely lectin-deficient (36) and which showed no change in melting temperature (Fig. 8*D*). Remarkably, when the ΔTip2 mutant of Crt was expressed in K42 cells (Fig. 8*B*, *bottom left*), it could not be detected within the PLC (Fig. 8*B*, *bottom right*). These findings reveal a previously unappreciated role for the arm domain of Crt in mediating its inclusion within the PLC.

DISCUSSION

The best characterized thiol oxidoreductase within the mammalian ER is PDI. Its four thioredoxin-like domains form a twisted U-shaped structure with active sites in the *a* and *a′* domains facing each other at the ends of the U (37). The primary substrate binding region has been mapped to the *b′* domain (38), which contains a hydrophobic pocket at the base of the U, well suited for interaction with nonnative protein substrates (37). However, hydrophobic patches are also evident near the active sites, and *in vitro* studies have demonstrated that the isolated *a* and *a′* domains can catalyze oxidation and reduction reactions with peptide and protein substrates (39), suggesting that they also possess weak substrate binding sites.

In contrast to PDI, the *b′* domain of ERp57 has become specialized for interaction with the arm domains of the lectin chaperones Cnx and Crt (29, 40). Instead of the hydrophobic pocket observed in PDI, the corresponding region of the ERp57 *b′* domain is charged, and residues that interact with the tip of the arm domain in Cnx and Crt, Lys-214, Lys-274, Arg-280, Asn-281, and Arg-282, have been mapped to the opposite side of the ERp57 *b′* domain (29, 40, 41). Therefore, rather than binding to substrates directly, it is widely believed that ERp57 is recruited by Cnx and Crt to the proximity of folding intermediates, which bear monoglucosylated *N*-linked glycans. This view is supported by the *in vitro* finding that the rate of oxidative refolding of monoglucosylated RNase B by ERp57 is dramatically accelerated by the presence of Cnx or Crt (6). Furthermore, studies in cell lines showed that when lectin-mediated interactions of Cnx and Crt with folding glycoproteins were prevented by castanospermine treatment, mixed disulfide complexes between several substrates and ERp57 were reduced or prevented (42, 43). However, the inability to detect transient mixed disulfides does not necessarily reflect loss of ERp57 function, and there have been no *in vivo* experiments that directly test whether Cnx or Crt are required for ERp57 to catalyze the oxidative folding of a substrate.

Our previous observation that ERp57 enhances the rate of disulfide formation within MHC class I H chains (12), coupled with the availability of ERp57-deficient cells that can be used to express mutant forms of the enzyme, provided an ideal oppor-

[3] M. Häuptle, E.-M. Frickel, and L. Ellgaard, unpublished data.

tunity to address the chaperone requirements for ERp57 function in living cells. We first showed that the rates of H chain disulfide formation were normal in Crt-deficient cells or in cells depleted of Cnx through RNA interference. This could be due to an ability of ERp57 to act on H chains independently of these chaperones, but it is also possible that the absence of Cnx or Crt permits access of other thiol oxidoreductases, which can replace ERp57 in catalyzing H chain disulfide formation. To distinguish between these possibilities, we made use of the R282A point mutant of ERp57, which does not interact with Cnx or Crt, as assessed by NMR and co-immunoisolation approaches, and demonstrated that it complements the slow oxidative folding phenotype of H chains in ERp57-deficient cells just as effectively as the wild type enzyme. Therefore, neither Cnx nor Crt is required for ERp57 to catalyze disulfide formation in the class I H chain substrate. Consistent with our finding, Jessop *et al.* (42) reported that, in an *in vitro* translation system, clusterin required the presence of ERp57 for efficient oxidative folding and that folding could still occur at a normal rate when interactions with Cnx or Crt were perturbed by treatment with castanospermine.

If Cnx and Crt are not required to bring ERp57 into the proximity of class I H chains, how does ERp57 gain access to H chains during oxidative folding? We propose that ERp57 is capable of recognizing newly synthesized H chains and some additional substrates directly. This notion is supported by the finding that the mixed disulfide conjugate between ERp57 and tapasin could be formed *in vitro* upon mixing recombinant components (44). Another example is clusterin, which, following *in vitro* translation in the presence of castanospermine, could still be detected in a noncovalent complex with ERp57 (42). By analogy to PDI, ERp57 may possess secondary substrate binding sites in the *a* and *a′* domains (38, 39, 45, 46). Consistent with this, Ellgaard and co-workers (5) have demonstrated that the isolated *a* and *a′* domains possess disulfide isomerase activity that is capable of reactivating disulfide-scrambled ribonuclease A *in vitro*. Furthermore, the recent crystal structure of the ERp57-tapasin conjugate revealed that, in addition to the expected disulfide cross-link between the two molecules, there was an extensive 1580 $Å^2$ interface that involved numerous contacts in the vicinity of the *a* and *a′* domain active sites of ERp57 (47).

We also examined the role of Cnx and Crt in the recruitment of ERp57 into the peptide loading complex. It has generally been thought that ERp57 enters the PLC mainly through interactions with Cnx or Crt, either via a preloading complex consisting of Cnx, ERp57, tapasin, and TAP (48) or through interactions with class I heterodimers in an H chain-β_2m-Crt-ERp57 complex (13). However, continuing the theme of direct ERp57-substrate interactions, we found that the K214A and R282A mutants of ERp57 that are impaired or lack interactions with Cnx and Crt, respectively, were still recruited into the PLC and formed conjugates with tapasin. Furthermore, we showed that ERp57 recruited in this manner retains functionality in stabilizing the PLC and promoting peptide loading of class I molecules although, in the case of R282A, somewhat less efficiently than observed for wild type ERp57. The reason for the lack of full functionality with the R282A mutant is unclear. However, a model of the PLC that incorporates the ERp57-tapasin crystal structure and known contacts between tapasin, H chain, Crt, and ERp57 predicts that the arm domain of Crt curves around the peptide-binding groove of class I to contact ERp57 (47). This may protect the nonnative class I molecule from reduction by ER thiol oxidoreductases or contribute to overall stability of the PLC, functions that would be lost with the R282A mutant. Our findings are consistent with those of Cresswell and co-workers (44), who found in the human system that ERp57 can be recruited into the PLC independently of incoming class I heterodimers and that ERp57-tapasin conjugates can form in the individual absence of Cnx or Crt. Thus, at both early and later stages in the biogenesis of mouse and human class I molecules, ERp57 can effect its functions without recruitment through the Cnx/Crt chaperone system.

We extended our analysis of ERp57 functions within the PLC by addressing whether it requires its thiol oxidoreductase activity to stabilize the PLC and promote peptide loading. Previous studies focusing on the redox activity of ERp57 have shown that when formation of the ERp57-tapasin conjugate is prevented by mutagenesis of cysteine 95 of tapasin, H chains in the PLC are partially reduced, indicating that the ERp57-tapasin conjugate may be involved in maintaining the oxidized state of the H chain during peptide loading (13). Subsequently, it was demonstrated that the disulfide proximal to the peptide-binding groove of the H chain is highly vulnerable to reduction by ERp57 and that tapasin, by forming the disulfide conjugate with ERp57, restrains the reductase activity of ERp57 (15). However, these studies did not delineate any positive role for ERp57 in peptide loading. Using ERp57-deficient cells, Garbi *et al.* (14) found that the PLC was unstable, that class I molecules left the loading complex more rapidly than in wild type cells, and that the efficiency of peptide loading and surface expression of $H\text{-}2K^b$ were reduced. It was proposed that the ERp57-tapasin conjugate is a key structural component that stabilizes class I molecules in the PLC, thereby facilitating peptide loading. Consistent with this model, Wearsch and Cresswell (16) demonstrated that recombinant tapasin alone was unable to recruit peptide-receptive class I molecules from cell lysates and facilitate peptide loading, whereas recombinant tapasin-ERp57 conjugates accomplished both of those functions. However, it remained unclear whether the enzymatic activity of ERp57 is required for its functions in stabilizing the PLC and promoting peptide loading.

Consequently, we mutated all active site cysteines of ERp57 except for Cys-57, which forms the disulfide conjugate with tapasin. Remarkably, this enzymatically inactive mutant, C60A/C406A/C409A, was indistinguishable from wild type ERp57 in fully supporting assembly of the PLC and the generation of normal levels of peptide-loaded class I molecules in total cell lysates and at the cell surface. These results clearly establish that the thiol oxidoreductase activity of ERp57 is dispensable for its functions within the PLC and that this enzyme acts as a structural component to maintain the integrity of the PLC. Our findings are consistent with the tapasin-ERp57 crystal structure, which showed that the *a* and *a′* domain active sites are buried in the interface with tapasin, rendering them inaccessible for catalysis of redox reactions other than the mixed disul-

fide with tapasin (47). Interestingly, the double mutant within the a' domain active site, C406A/C409A, failed to form the conjugate with tapasin and was unable to rescue the defects in class I biogenesis observed in ERp57$^{-/-}$ cells. The unexpected behavior of this mutant has also been documented previously in the human system (13). As shown in the tapasin-ERp57 structure, the a' domain active site is involved in multiple contacts with tapasin and hence contributes significantly to binding (47). However, this requirement for Cys-406/Cys-409 is obviated in the absence of the escape pathway in the triple mutant.

While this manuscript was in preparation, Cresswell and coworkers (49) reported that when the C60A/C406A/C409A mutant of human ERp57 was expressed in cells stably knocked down for endogenous ERp57, it fully supported PLC assembly and the generation of stable, peptide-loaded human HLA*B4402 molecules. Although consistent with our findings in the mouse system, the interpretation of their results is complicated by the presence of residual conjugate between tapasin and endogenous wild type ERp57 that remained following the ERp57 knockdown.

In the absence of any enzymatic role, how does ERp57 stabilize the PLC? It has been suggested that ERp57, through its interaction with Crt, may stabilize Crt-associated class I molecules within the PLC (49). As mentioned above, we examined this possibility by disrupting the ERp57-Crt interaction either through the ERp57 R282A mutation (Figs. 6 and 7) or by mutating the tip of the arm domain of Crt by point mutation (D258N) or by replacement with residues from *S. cerevisiae* Cnx (Fig. 8). Despite the loss of the Crt-ERp57 interaction, PLC assembly was normal, and there was only a modest reduction in surface class I expression in the case of the R282A mutant. This is in marked contrast to the PLC instability and low surface expression of class I associated with ERp57 deficiency (14). We favor the suggestion put forward by Garbi *et al.* (14) that ERp57 conjugate formation with tapasin influences the conformation of tapasin, rendering it competent for association with H chain-β_2m heterodimers and recruiting them into the PLC. This notion is supported by the finding that the tapasin-ERp57 conjugate, but not tapasin alone, can recruit peptide-receptive class I molecules from cell lysates (16). Furthermore, the extensive 1580 Å^2 interface between tapasin and ERp57 suggests that ERp57 exerts a significant influence on the conformations that tapasin can assume (47). Given that the class I binding site on tapasin has recently been shown to be combinatorial in nature (47), such an influence of ERp57 is likely to impact the tapasin-class I association. In the future, it will be of considerable interest to address this issue using biophysical approaches to probe the conformational states of both tapasin-ERp57 and free tapasin. The concept of ERp57 as a structural rather than catalytic component of the PLC is reminiscent of the noncatalytic roles that have been demonstrated for PDI, namely as the β subunit of prolyl 4-hydroxylase (50) and a component of the microsomal triglyceride transfer protein complex (51).

During the course of these studies, we noted that disruption of the Crt-ERp57 interaction not only had minimal effects on ERp57 within the PLC but also failed to perturb the levels of Crt within the loading complex (Fig. 8*A*). This returned us to the ongoing debate as to what interactions are critical for recruitment of Crt into the PLC. It is a widely held view that the interaction of Crt with class I H chains and with the PLC is mediated largely through its ability to bind monoglucosylated oligosaccharides on H chains. Inhibition of the formation of monoglucosylated oligosaccharides on class I H chains, either by treating the cells with the glucosidase inhibitor castanospermine (52) or by removing the oligosaccharide moiety in the α_1 domain of the H chain (53), reduced Crt association with class I molecules. *In vitro* experiments using immobilized monoglucosylated free H chains also showed that the glycan on class I H chains was necessary and sufficient for the binding of Crt (33). However, this view was recently called into question by our recent demonstration that lectin-deficient mutants of Crt retained full ability to associate with class I molecules and complement all class I biosynthetic defects associated with Crt deficiency (24). Since it was apparent that disruption of the lectin and ERp57-binding functions of Crt individually was insufficient to prevent its interactions with class I molecules and its incorporation into the PLC, we made the double mutant Y128A/D258N, which lacks both functions. Surprisingly, this mutant was incorporated into the PLC, indicating that a third mode of interaction was sufficient for Crt recruitment. Both Crt and Cnx possess the ability to associate via polypeptide-based interactions with nonnative protein conformers both *in vitro* (54, 55) and in living cells. This function resides in the globular lectin domain and endows these chaperones with the ability to suppress protein aggregation *in vitro* under physiological conditions (24, 25, 56). We propose that in the absence of other modes of association, such polypeptide-based interactions are sufficient to effect Crt functions in class I biogenesis. Interestingly, we found that a variant of Crt with a truncated arm domain that lacks ERp57 binding ability but retains full lectin function was not incorporated into the PLC. *In vitro* experiments with the analogous Cnx variant revealed that it retains its polypeptide binding function as measured with small peptides, but its binding affinity for unfolded proteins is reduced (57). This is consistent with a model wherein nonnative proteins, such as H chain-β_2m heterodimers, enter the cavity formed between the globular and arm domains of Crt. This permits lectin- and polypeptide-based interactions within the globular domain to occur, whereas the arm domain sterically impedes substrate dissociation. Based on the inability of the truncated arm variant of Crt to be detected in the PLC, this latter function may contribute significantly to the overall binding interaction with assembling class I molecules.

Acknowledgments—We thank Drs. Natalio Garbi and Günter Hämmerling for kindly providing ERp57-deficient fibroblasts; Micha Häuptle, Dr. Eva-Maria Frickel, and Dr. Lars Ellgaard for the generous gift of cDNA encoding Crt with the S. cerevisiae tip sequence; Dr. Young Yang for anti-TAP1 antiserum; Dr. Marek Michalak for Crt-deficient K42 cells; and Dan Chapman for performing flow cytometry analyses.

REFERENCES

1. Garbi, N., Tanaka, S., van den Broek, M., Momburg, F., and Hammerling, G. J. (2005) *Immunol. Rev.* **207,** 77–88
2. Peaper, D. R., and Cresswell, P. (2008) *Annu. Rev. Cell Dev. Biol.* **24,**

343–368
3. Ellgaard, L., and Ruddock, L. W. (2005) *EMBO Rep.* **6,** 28–32
4. Antoniou, A. N., Ford, S., Alphey, M., Osborne, A., Elliott, T., and Powis, S. J. (2002) *EMBO J.* **21,** 2655–2663
5. Frickel, E. M., Frei, P., Bouvier, M., Stafford, W. F., Helenius, A., Glockshuber, R., and Ellgaard, L. (2004) *J. Biol. Chem.* **279,** 18277–18287
6. Zapun, A., Darby, N. J., Tessier, D. C., Michalak, M., Bergeron, J. J., and Thomas, D. Y. (1998) *J. Biol. Chem.* **273,** 6009–6012
7. Helenius, A., and Aebi, M. (2004) *Annu. Rev. Biochem.* **73,** 1019–1049
8. Williams, D. B. (2006) *J. Cell Sci.* **119,** 615–623
9. Frickel, E. M., Riek, R., Jelesarov, I., Helenius, A., Wuthrich, K., and Ellgaard, L. (2002) *Proc. Natl. Acad. Sci. U. S. A.* **99,** 1954–1959
10. Leach, M. R., Cohen-Doyle, M. F., Thomas, D. Y., and Williams, D. B. (2002) *J. Biol. Chem.* **277,** 29686–29697
11. Schrag, J. D., Bergeron, J. J., Li, Y., Borisova, S., Hahn, M., Thomas, D. Y., and Cygler, M. (2001) *Mol. Cell* **8,** 633–644
12. Zhang, Y., Baig, E., and Williams, D. B. (2006) *J. Biol. Chem.* **281,** 14622–14631
13. Dick, T. P., Bangia, N., Peaper, D. R., and Cresswell, P. (2002) *Immunity* **16,** 87–98
14. Garbi, N., Tanaka, S., Momburg, F., and Hammerling, G. J. (2006) *Nat. Immunol.* **7,** 93–102
15. Kienast, A., Preuss, M., Winkler, M., and Dick, T. P. (2007) *Nat. Immunol.* **8,** 864–872
16. Wearsch, P. A., and Cresswell, P. (2007) *Nat. Immunol.* **8,** 873–881
17. Nakamura, K., Zuppini, A., Arnaudeau, S., Lynch, J., Ahsan, I., Krause, R., Papp, S., De Smedt, H., Parys, J. B., Muller-Esterl, W., Lew, D. P., Krause, K. H., Demaurex, N., Opas, M., and Michalak, M. (2001) *J. Cell Biol.* **154,** 961–972
18. Smith, M. H., Parker, J. M., Hodges, R. S., and Barber, B. H. (1986) *Mol. Immunol.* **23,** 1077–1092
19. Ozato, K., Mayer, N. M., and Sachs, D. H. (1982) *Transplantation* **34,** 113–120
20. Ribaudo, R. K., and Margulies, D. H. (1992) *J. Immunol.* **149,** 2935–2944
21. Ozato, K., and Sachs, D. H. (1981) *J. Immunol.* **126,** 317–321
22. Lemke, H., Hammerling, G. J., and Hammerling, U. (1979) *Immunol. Rev.* **47,** 175–206
23. Suh, W. K., Derby, M. A., Cohen-Doyle, M. F., Schoenhals, G. J., Fruh, K., Berzofsky, J. A., and Williams, D. B. (1999) *J. Immunol.* **162,** 1530–1540
24. Ireland, B. S., Brockmeier, U., Howe, C. M., Elliott, T., and Williams, D. B. (2008) *Mol. Biol. Cell* **19,** 2413–2423
25. Danilczyk, U. G., and Williams, D. B. (2001) *J. Biol. Chem.* **276,** 25532–25540
26. Ho, S. N., Hunt, H. D., Horton, R. M., Pullen, J. K., and Pease, L. R. (1989) *Gene* **77,** 51–59
27. Zheng, L., Baumann, U., and Reymond, J. L. (2004) *Nucleic Acids Res.* **32,** e115
28. Tolstrup, A. B., Duch, M., Dalum, I., Pedersen, F. S., and Mouritsen, S. (2001) *Gene* (*Amst.*) **263,** 77–84
29. Kozlov, G., Maattanen, P., Schrag, J. D., Pollock, S., Cygler, M., Nagar, B., Thomas, D. Y., and Gehring, K. (2006) *Structure* **14,** 1331–1339
30. Bartels, c., Xia, T. H., Billeter, M., Güntert, P., and Wüthrich, K. (1995) *J. Biomol. NMR* **6,** 1–10
31. Gao, B., Adhikari, R., Howarth, M., Nakamura, K., Gold, M. C., Hill, A. B., Knee, R., Michalak, M., and Elliott, T. (2002) *Immunity* **16,** 99–109
32. Walker, K. W., and Gilbert, H. F. (1997) *J. Biol. Chem.* **272,** 8845–8848
33. Wearsch, P. A., Jakob, C. A., Vallin, A., Dwek, R. A., Rudd, P. M., and Cresswell, P. (2004) *J. Biol. Chem.* **279,** 25112–25121
34. de Virgilio, C., Burckert, N., Neuhaus, J. M., Boller, T., and Wiemken, A. (1993) *Yeast* **9,** 185–188
35. Parlati, F., Dominguez, M., Bergeron, J. J., and Thomas, D. Y. (1995) *J. Biol. Chem.* **270,** 244–253
36. Thomson, S. P., and Williams, D. B. (2005) *Cell Stress Chaperones* **10,** 242–251
37. Tian, G., Xiang, S., Noiva, R., Lennarz, W. J., and Schindelin, H. (2006) *Cell* **124,** 61–73
38. Klappa, P., Ruddock, L. W., Darby, N. J., and Freedman, R. B. (1998) *EMBO J.* **17,** 927–935
39. Darby, N. J., Penka, E., and Vincentelli, R. (1998) *J. Mol. Biol.* **276,** 239–247
40. Russell, S. J., Ruddock, L. W., Salo, K. E., Oliver, J. D., Roebuck, Q. P., Llewellyn, D. H., Roderick, H. L., Koivunen, P., Myllyharju, J., and High, S. (2004) *J. Biol. Chem.* **279,** 18861–18869
41. Maattanen, P., Kozlov, G., Gehring, K., and Thomas, D. Y. (2006) *Biochem. Cell Biol.* **84,** 881–889
42. Jessop, C. E., Chakravarthi, S., Garbi, N., Hammerling, G. J., Lovell, S., and Bulleid, N. J. (2007) *EMBO J.* **26,** 28–40
43. Molinari, M., and Helenius, A. (1999) *Nature* **402,** 90–93
44. Peaper, D. R., Wearsch, P. A., and Cresswell, P. (2005) *EMBO J.* **24,** 3613–3623
45. Darby, N. J., and Creighton, T. E. (1995) *Biochemistry* **34,** 11725–11735
46. Koivunen, P., Salo, K. E., Myllyharju, J., and Ruddock, L. W. (2005) *J. Biol. Chem.* **280,** 5227–5235
47. Dong, G., Wearsch, P. A., Peaper, D. R., Cresswell, P., and Reinisch, K. M. (2009) *Immunity* **30,** 21–32
48. Diedrich, G., Bangia, N., Pan, M., and Cresswell, P. (2001) *J. Immunol.* **166,** 1703–1709
49. Peaper, D. R., and Cresswell, P. (2008) *Proc. Natl. Acad. Sci. U. S. A.* **105,** 10477–10482
50. Koivu, J., Myllyla, R., Helaakoski, T., Pihlajaniemi, T., Tasanen, K., and Kivirikko, K. I. (1987) *J. Biol. Chem.* **262,** 6447–6449
51. Wetterau, J. R., Combs, K. A., McLean, L. R., Spinner, S. N., and Aggerbeck, L. P. (1991) *Biochemistry* **30,** 9728–9735
52. Sadasivan, B., Lehner, P. J., Ortmann, B., Spies, T., and Cresswell, P. (1996) *Immunity* **5,** 103–114
53. Harris, M. R., Yu, Y. Y., Kindle, C. S., Hansen, T. H., and Solheim, J. C. (1998) *J. Immunol.* **160,** 5404–5409
54. Ihara, Y., Cohen-Doyle, M. F., Saito, Y., and Williams, D. B. (1999) *Mol. Cell* **4,** 331–341
55. Saito, Y., Ihara, Y., Leach, M. R., Cohen-Doyle, M. F., and Williams, D. B. (1999) *EMBO J.* **18,** 6718–6729
56. Leach, M. R., and Williams, D. B. (2004) *J. Biol. Chem.* **279,** 9072–9079
57. Brockmeier, A., Brockmeier, U., and Williams, D. B. (2008) *J. Biol. Chem.* **284,** 3433–3444